

High-Resolution Array Devices via Insulating Pattern Definition Layer Transferred by UV-Adhesive Stamp

Xudong Jiang^{#1}, Jie Li^{#1}, Zunxian Yang^{*,1,2}, Yue Chen¹, Luxi Yuan¹, Wenxin Tang¹,
Yuting Bai¹, Jiajie Hong¹, Benfang Liu¹, Zheyu Zhou¹, Runsen Yu¹, Wenxin Zhang¹,
Shangwei Ye¹, Zhiqian Wei¹, Zhezhou Fang¹, Jinzhu Gao¹, Zhiyu Yuan¹, Shunchang
Cheng¹, Yuhan Meng¹, Zhiqi Lin¹, Tailiang Guo^{1,2}, Zhenzhen Weng³, Yongyi Chen³

¹National & Local United Engineering Research Center of Flat Panel Display
Technology, Fuzhou University, Fuzhou 350108, P. R. China.

²Mindu Innovation Laboratory, Fujian Science & Technology Innovation Laboratory
For Optoelectronic Information of China, Fuzhou, 350108, P.R. China

³Department of Physics, School of Physics and Information Engineering, Fuzhou
University, Fuzhou 350108, P. R. China.

Supporting Information

[#]They made equal contribution to this manuscript

* Corresponding author should be addressed. Tel.: +86 591 8789 3299; Fax: +86 591 8789 2643
E-mail: yangzunxian@hotmail.com (Z. Yang)

Captions

Figure S1 Swelling phenomenon observed after spin-coating PMMA in chlorobenzene solvent on a PDMS substrate.

Figure S2 (a) AFM measurement result of the cylindrical height of the UV-adhesive stamp; **(b)** AFM-measured pore depth of the microporous film prepared from 10 mg/mL PMMA and filled with HIL; **(c)** 2D and 3D topographic images of PMMA microporous films prepared by rigid substrate stamps; **(d)** 2D and 3D topographic images of PMMA microporous films prepared by flexible substrate stamps.

Figure S3 (a-b) Measurement of Young's modulus on the PDMS surface; **(c-d)** Plot of the discrete distribution of Young's modulus within a local area on the PDMS surface.

Figure S4 (a) Schematic illustration of pressure distribution in the rigid-soft composite stamp during the pattern transfer process; **(b)** Schematic illustration of pressure distribution in a stamp with a thick flexible substrate during the pattern transfer process.

Figure S5 (a) SEM images of a PMMA microporous film from a low-magnification overview to progressively higher magnifications; **(b)** Photoluminescence images of the microporous structures infused with quantum dots from a low-magnification overview to progressively higher magnifications; **(c)** Measurement of the actual effective area of the transferred PMMA microporous film.

Figure S6 (a) Optical microscopy image of the uniform filling and light emission of quantum dots within the micropores; **(b)** Microscopic measurement results of pixel

size.

Figure S7 Pixel count on a 25.4 μm diagonal line, representing approximately 1/1000 of the pixel count per inch.

Figure S8 (a) and (b) Wetting behavior of PEDOT: PSS on the PMMA surface before and after hydrophilic treatment.

Figure S9 (a) Schematic diagram of the high-resolution device structure and the internal structure of the microporous film; **(b)** Energy band diagrams of the blocking and emissive regions, and a schematic illustration of the electron-hole recombination mechanism.

Figure S10 (a) Circuit schematic of the high-resolution device without an insulating layer, showing leakage paths; **(b)** Circuit schematic illustrating the blocking effect of the insulating layer between pixels.

Figure S11 (a) Comparison of fluorescence spectra between patterned and non-patterned devices; **(b)** Comparison of fluorescence lifetime between patterned and non-patterned devices; **(c)** Plot of the chromaticity coordinates for a set of high-resolution devices; **(d)** Electroluminescence spectra of the high-resolution device at applied voltages from 4 V to 8 V.

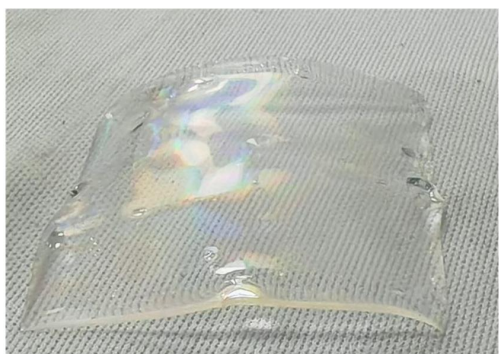


Figure S1

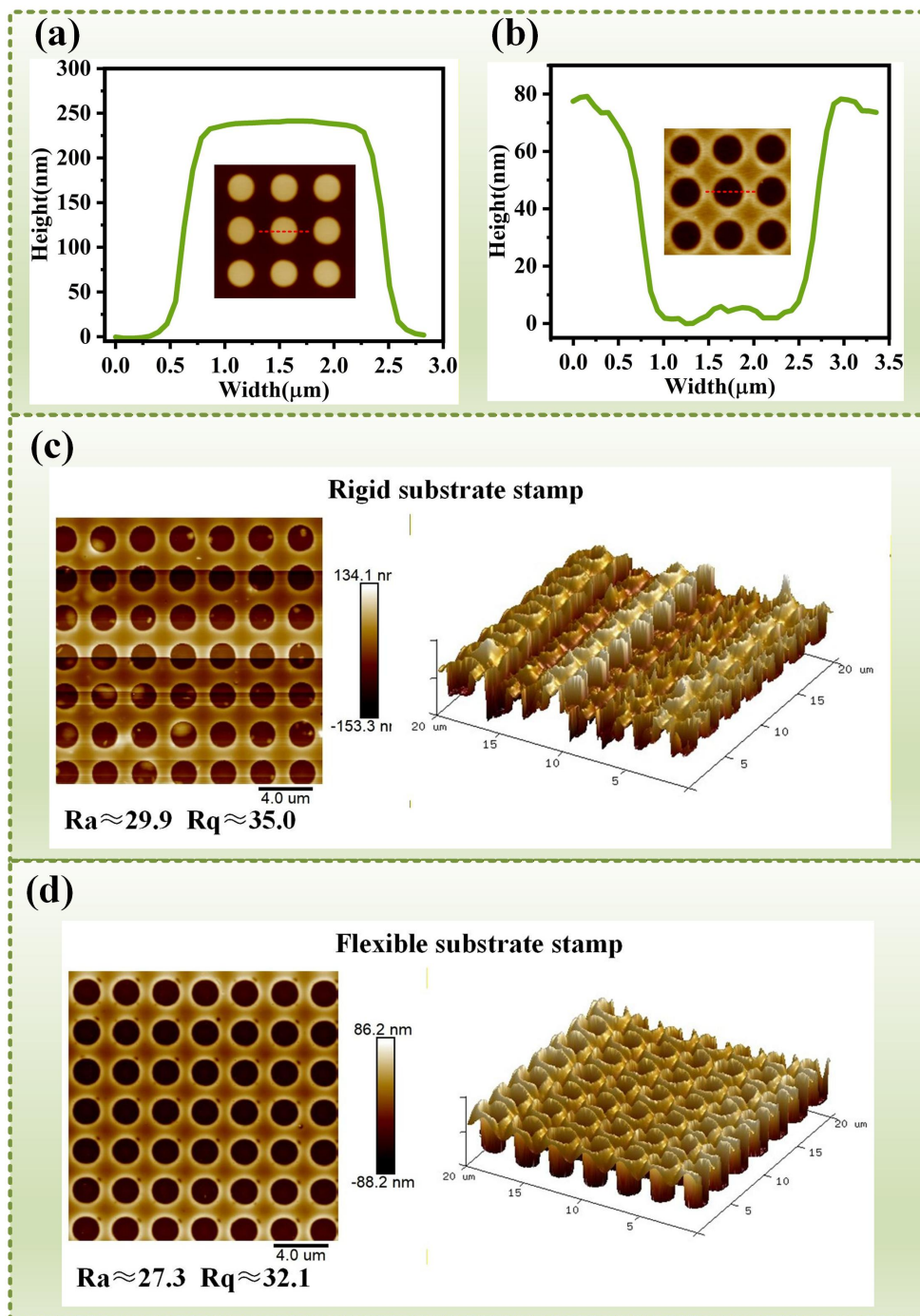


Figure S2

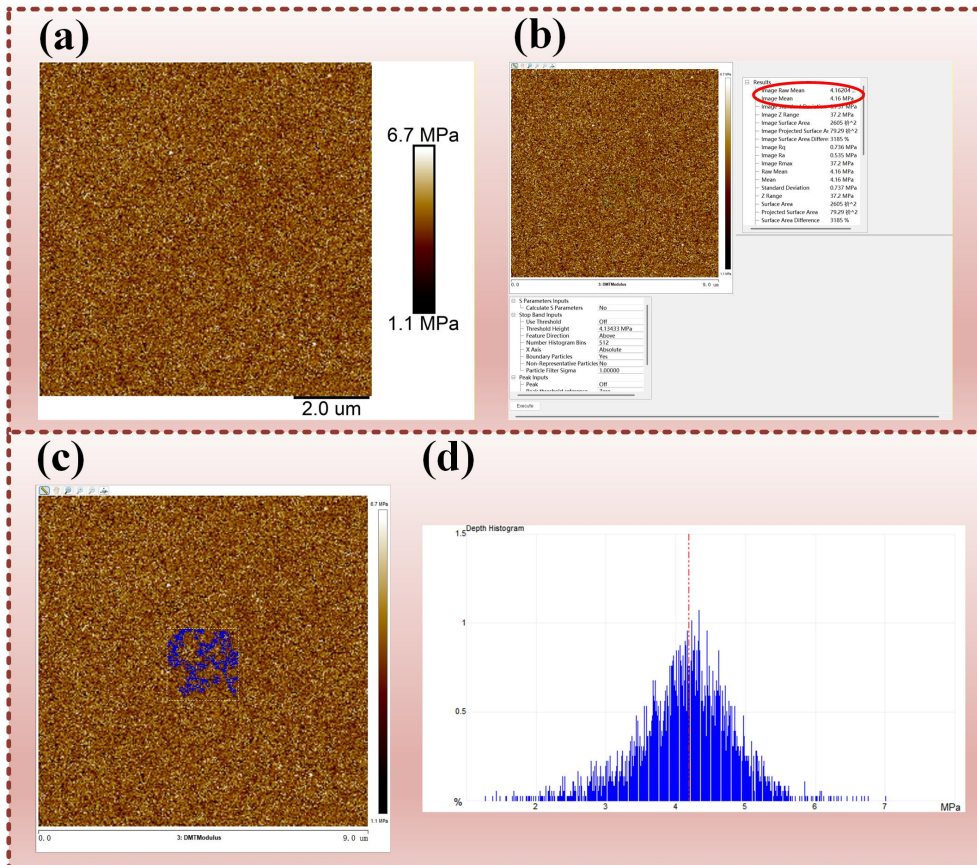
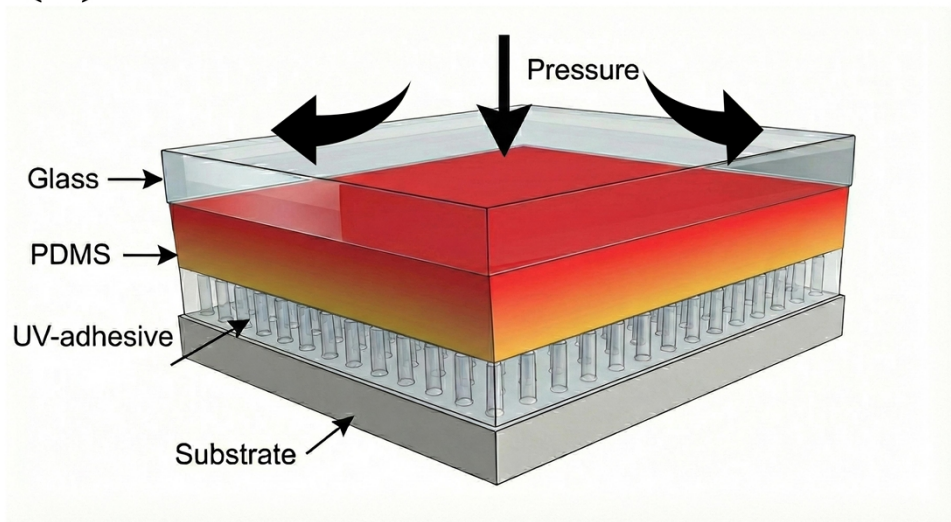


Figure S3

(a)



(b)

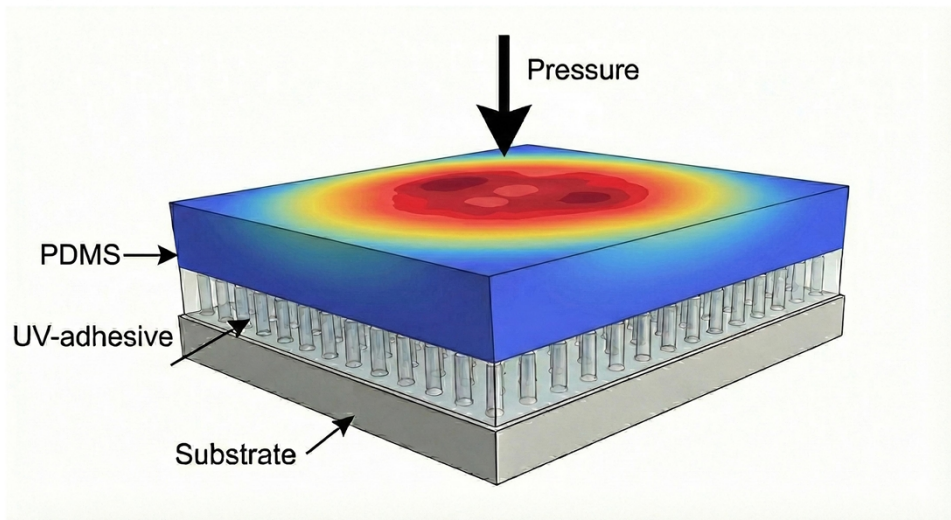


Figure S4

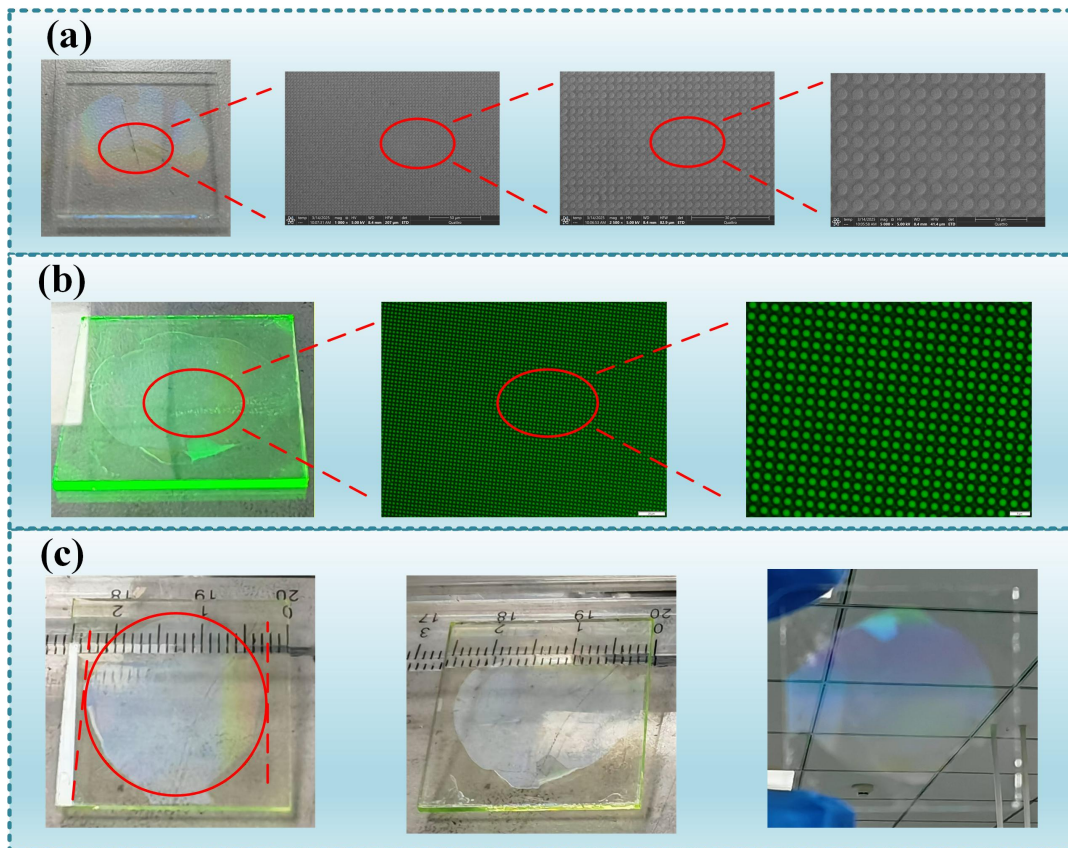


Figure S5



(a)



(b)

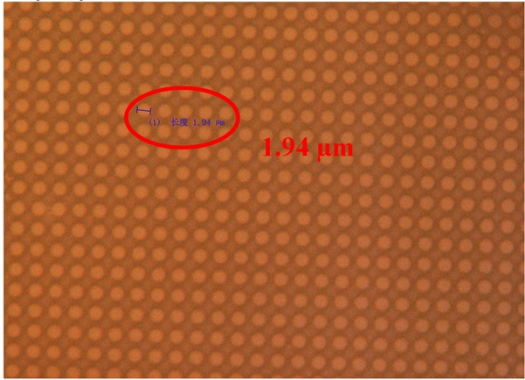


Figure S6

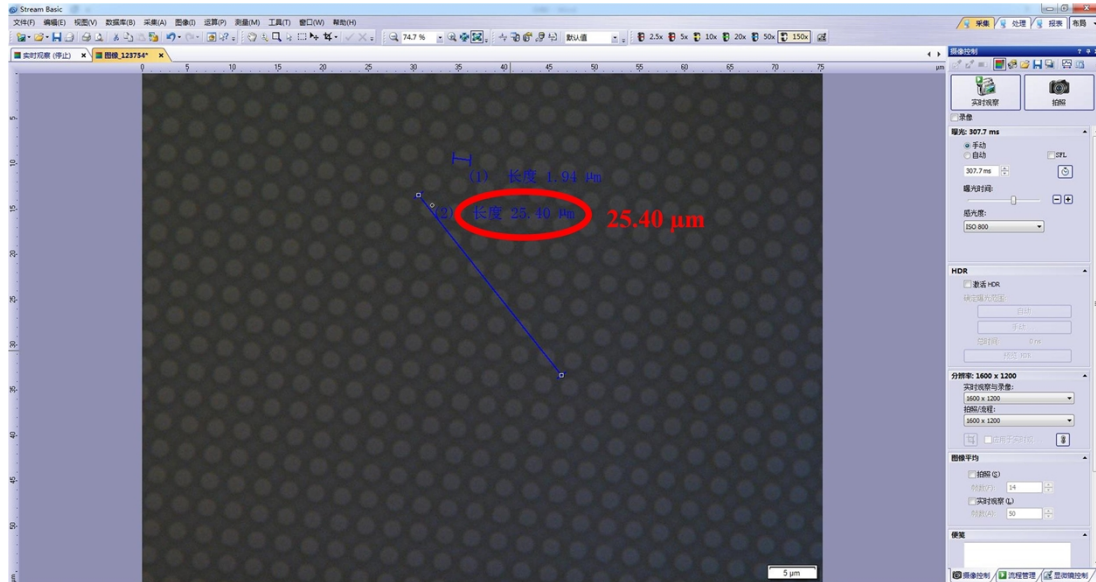


Figure S7

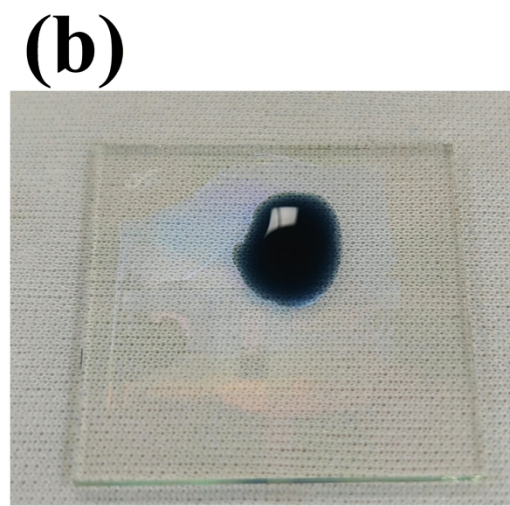
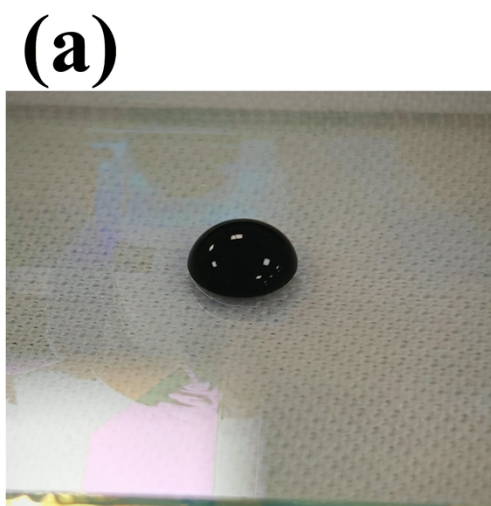


Figure S8

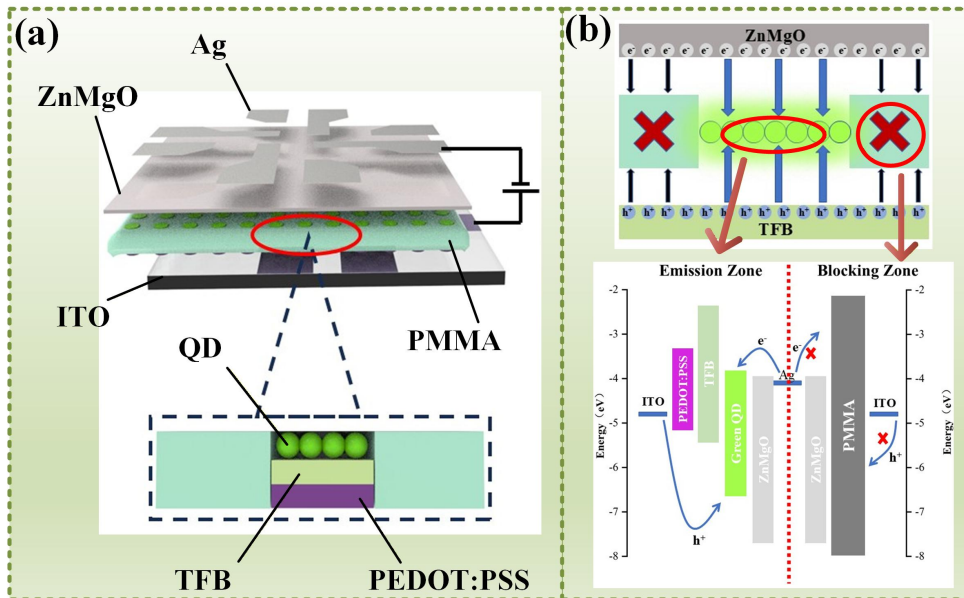


Figure S9

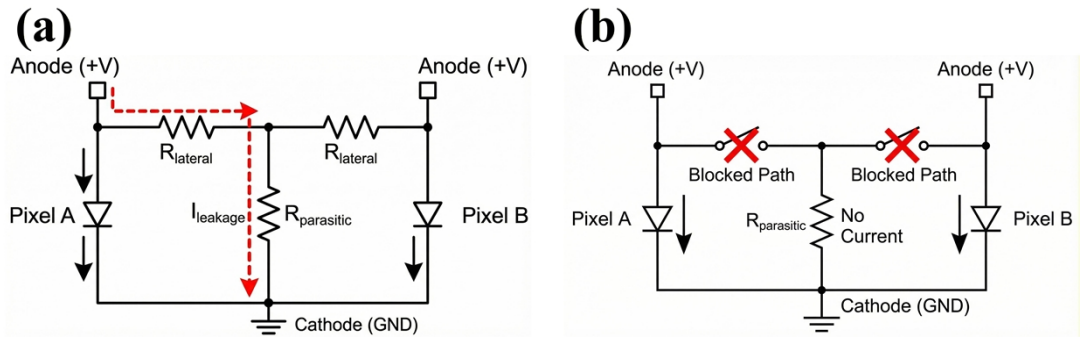


Figure S10

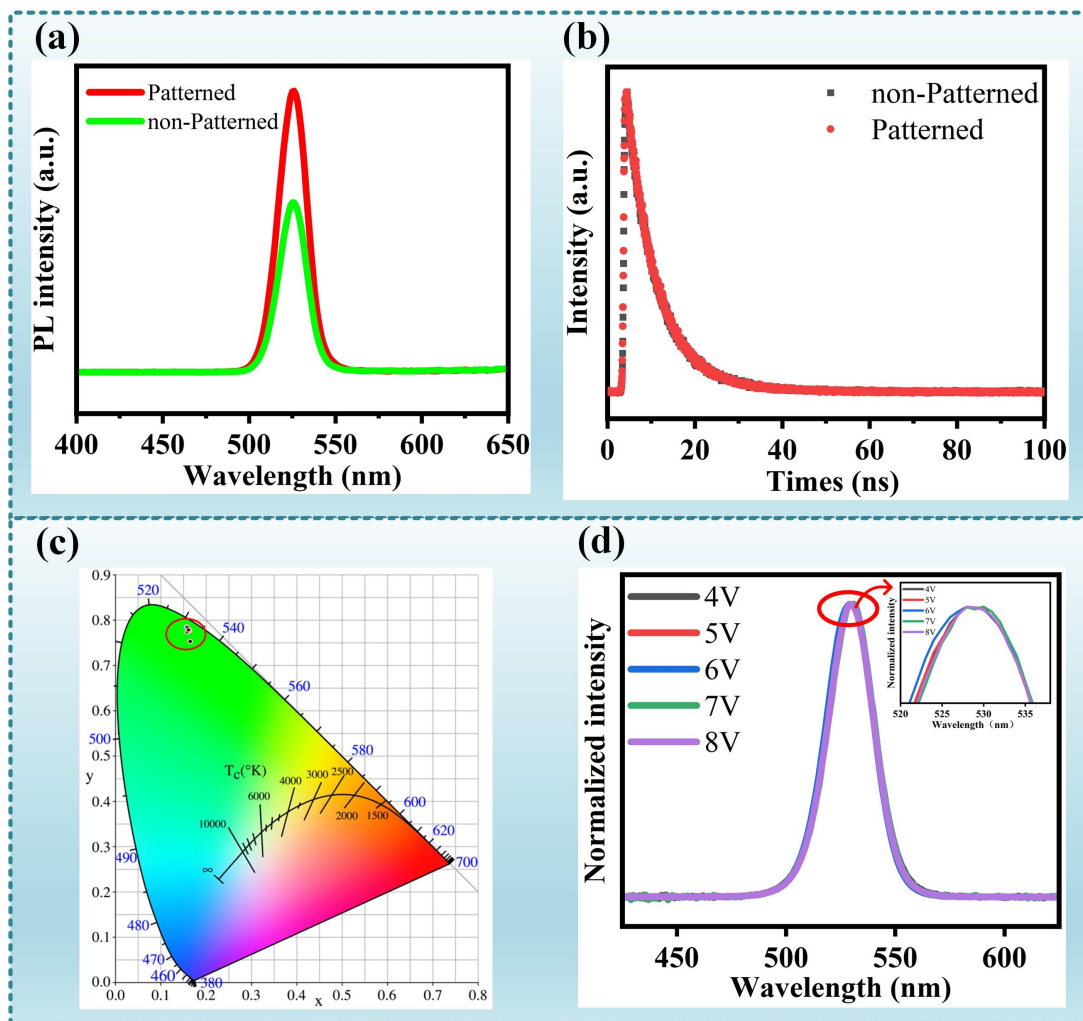


Figure S11